On the tails of distributions of annual peak flow

Witold G. Strupczewski, Krzysztof Kochanek, Iwona Markiewicz, Ewa Bogdanowicz, Stanislaw Weglarczyk and Vijay P. Singh

ABSTRACT

This study discusses an application of heavy-tailed distributions to modelling of annual peak flows in general and of Polish data sets in particular. One- and two-shape parameter heavy-tailed distributions are obtained by transformations of random variables. The correct selection of a flood frequency model with emphasis on heavy-tailed distribution discrimination is then discussed. If a distribution is wrongly assumed, the error, in the upper quantile, arising as a result, depends on the method of parameter estimation and is shown analytically for three methods. Asymptotic and sampling values (got by simulation) were assessed for the pair log-Gumbel (*LG*) as a false distribution and log-normal (*LN*) as a true distribution. Comparing the upper quantiles of various distributions with the same values of moments, it is found that heavy-tailed distributions do not consistently provide higher flood frequency estimates than do soft-tailed distributions. Based on *L*-moment ratio diagrams and the test of linearity on log–log plots, it is concluded that Polish datasets of annual peak flows should be modelled using soft-tailed distributions, such as the three-parameter Inverse Gaussian, rather than heavy-tailed distributions.

Key words | bias, heavy tail, hydrological extremes, *L*-moments, parameters' estimation of probability distribution, quantiles

Witold G. Strupczewski (corresponding author)
Krzysztof Kochanek
Iwona Markiewicz
Water Resources Department,
Institute of Geophysics,
Polish Academy of Sciences,
Ksiecia Janusza 64, 01-452 Warsaw,
Poland
E-mail: *wgs@igf.edu.pl*

Ewa Bogdanowicz
Institute of Meteorology and Water Management,
Podlesna 61, 01-673 Warsaw,
Poland

Stanislaw Weglarczyk
Faculty of Environmental Engineering,
Cracow University of Technology
Warszawska 24, 31-155 Cracow,
Poland

Vijay P. Singh
Department of Biological and Agricultural Engineering & Department of Civil & Environmental Engineering,
Texas A & M University, Scoates Hall,
2117 TAMU, College Station,
Texas 77843-2117,
USA

INTRODUCTION

Statistics of extremes has played an important role in the design and management of water resources. The classical extreme value theory is built on the assumption that observations in the time series are independent and identically distributed (i.i.d.). The cornerstone of the theory is that "three types" of distributions can arise as limiting distributions of extremes in random samples, i.e., Gumbel, Fréchet and Weibull. They are combined into the Generalized Extreme Value (*GEV*) distribution, which has been widely used for modelling the distribution of flood peaks for both at-site and regional cases. The main objection to this approach is that hydrological processes rarely produce observations that are i.i.d. and that their number in each observation period is small. The rate of convergence of an extreme value distribution with increasing number of i.i.d. events towards the theoretical extreme value distribution is not particularly rapid (Makkonen 2008). This then opens the room for using alternative distribution families, provided they fit the data better.

In Flood Frequency Analysis (FFA), a probability density function (PDF) is selected more or less subjectively from among positively skewed PDFs of continuous type. Some of these distributions have been introduced because of their suitability to model different shapes of histogram or perhaps simply because they had not been used before (Cunnane 1989). A few of the distributions are supported on the basis of deductive reasoning about the genesis of floods. Since the theoretical arguments advanced for the purpose can be easily undermined, empirical suitability plays a much larger role in the distribution choice than a priori reasoning. Obviously, the

doi: 10.2166/nh.2011.062

effect of the model selection is more pronounced and critical in the upper tail of the distribution which is of greater significance in hydrological designs.

Nowadays there is a growing consensus that hydrological extremes are heavy-tail distributed which is inherited from presumably heavy tailed maximum precipitation. El Adlouni *et al.* (2008) proposed a bunch of methods for tail discrimination which can help decide whether a given sample should be described by a heavy-tailed distribution. The focus of the present study is on the applicability of heavy-tailed distributions to modelling of annual peak flows in general and of Polish data sets in particular. The present views on the causes of the appearance of heavy tailed (inverse-power) distributions in nature are briefly presented in the next section. A variety of heavy-tailed distribution functions with one or two shape parameters can be derived from transformation of some soft-tailed distributed variables or both soft- and heavy-tailed distribution functions (section "Candidate heavy-tailed distributions for flood frequency analysis").

Hydrological records are too short to provide sufficient evidence for heavy-tailed properties of extremes. The evidence obtained by "regional averaging" of distribution parameters of annual hydrological maxima (Hosking & Wallis 1997) (i.e., a trade-off between space and time) can be undermined according to Klemeš (2000) as an artefact of using *L*-moment method (LMM). Hence, a variety of both thin- and thick-tailed distributions are equal as alternative models for a given sample. Our findings on the selection of the model that best fits a set of observations are briefly presented in the section "Model selection". Finally, the selection procedure recently developed by El Adlouni *et al.* (2008) is adopted. The possibility of correct identification of a PDF in the case of normal hydrological sample sizes is small even in the ideal case when the set of alternative PDFs contains the true (T) distribution function. Therefore, in reality, one deals with a hypothetical PDF, called here the false distribution function (F), which somewhat differs from the true one (T). This results in error (bias) in statistical characteristics of the distribution (section "Model error"). Its asymptotic and sampling values (got by simulation) for upper quantiles are assessed for the pair log-Gumbel (*LG*) as a false model and log-normal (*LN*) as a true model.

The next section deals with the evaluation of practical importance of replacing thin-tailed distributions by heavy-tailed distributions for hydrologic design. Results of two estimation methods, namely moments and *L*-moments, for the same summary statistics values used for distribution fitting, are discussed. The title of the penultimate section "Looking for heavy-tailed distributions of the Polish rivers flow data" is self-explanatory. The conventional *L*-moment ratio diagrams for two- and three-parameter distributions and the two-step procedure of model selection (El Adlouni *et al.* 2008) are applied. Finally, the last section is for conclusions and recommendations.

CAUSES OF INVERSE-POWER DISTRIBUTION IN NATURE

Many geophysical phenomena, because of their complexity, manifest non-regular and chaotic behaviour. It appears, however, that statistically some observational distributions and patterns reveal that their nature is not purely random. The patterns have a fractal or multi-fractal structure and distributions resemble a long-tail of inverse power form. The observations include (after Czechowski 2001 and Malamud & Turcotte 2006) streamflows, topography, river networks, precipitation, clouds, forest fires, landslides, rock fragments, mineral deposits, volcanic eruptions, turbulent eddies, crack populations, fault distributions, asteroid impacts, and magnitude frequency. The revelation from these facts is quite surprising; it testifies to some universality of behaviour of complex systems irrespective of the processes (physical, chemical, biological or economical) they describe. The widespread appearance of inverse-power like distributions in nature and human activity raises self-evident questions about the reasons. There are many mechanisms that produce power laws. A complex review of all these mechanisms is given by Newman (2005), while some simple algebraic methods are quoted by El Adlouni *et al.* (2008). The cause of inverse-power-like forms can be explained both by a nonlinear approach (Czechowski 2001) and a privilege approach (Czechowski 2005). There is a relation between these two approaches, however.

In the first approach, the structure of the medium, or the behaviour of intrinsic processes, is purely random at the lowest description level, i.e., it may be characterized by purely random distributions, such as Poisson, exponential

or Gaussian. Physical phenomena are modelled as a kind of black box g that transforms input variables $\mathbf{x}$ into an output variable $y = g(\mathbf{x})$ that is of interest in a given phenomenon. The intrinsic structure of the model or unknown parameters is used as input random variables. An amazingly wide class of non-linear models transforms random (exponential) distributions into long tail distributions. The class includes increasing functions between power one ($g(x) = x^k$ for sufficiently large k), exponential one and those that increase very rapidly along a vertical asymptote. In the case of more non-linear functions $g(x)$, the inverse-power-like forms of distribution functions appear for sufficiently large values of y. When the models are represented by differential equations, the degree of non-linearity of equations may be lower. Chaotic phenomena are caused by non-linearities of the model, and therefore non-linearities can lead to inverse power distributions (see McCauley 1995).

In the second approach, the inverse power behaviour is derived using the privilege concept (where the privilege means the susceptibility of the state of the system to a change). Long tails mean an excess of large events in comparison with purely random distributions as the Poisson, exponential or normal. This suggests that during the evolution of the system, large events are in some way privileged.

If the inverse power forms of distribution functions appear for large events, i.e., the form of right tail for large y is $\lim_{y\to\infty} P(Y \geq y) = \lim_{y\to\infty} \bar{F}(y) \sim y^{-\alpha}$, then moments of the order r higher than $(\alpha + 1)$ do not exist.

CANDIDATE HEAVY-TAILED DISTRIBUTIONS FOR FFA

There is a belief among hydrologists that the extreme hydrological phenomena are best described by heavy-tailed distributions. In fact, there is no strict definition as to which distributions are heavy tailed, but one can assume that such distributions are characterised by the restriction with respect to the existence of theoretical moments, whereas moments calculated for a sample are always finite. That is why heavy-tailed distributions are often identified with limited-existence-moment distributions (LEM) (e.g., Strupczewski *et al.* 2005). An alternative definition of heavy-tailed distributions based on the fourth central moment was presented by El Adlouni *et al.* (2008) which says that $C_k > 3$, where C_k is the coefficient of kurtosis. Then all distributions commonly used in FFA would be classified as heavy-tailed.

Various heavy-tailed distribution functions can be obtained either by non-parametric transformation of some soft-tailed distributed variables (x) or by a parametric transformation of both soft- and heavy- distributions. The common non-parametric transformation functions (T) $y = g(x)$ are the exponential function $y = \exp(x)$ and the inverse of x: $y = x^{-1}$ The exponential transformation is applicable both to unbounded variables, i.e. with support $x \in (-\infty, +\infty)$, and to a lower bounded variable, i.e., $x \in [\epsilon_x, +\infty)$ (Table 1). Note that in each case it would transform a soft-tailed distributed variable into a heavy-tailed distributed variable. Also, from the normal distribution one gets log-normal distribution, which is only on the edge between PDFs having moments and LEM PDFs. However, taking another symmetric distribution, namely the logistic (Table 1), one can see that the same transformation results in a heavy-tailed distribution. In the case of a light-tailed lower-bounded distribution, such as Pearson (3) or three-parameter Inverse Gaussian (Tweedie 1957; Strupczewski *et al.* 2001*b*), the products of this transformation, the heavy-tailed log-Pearson (3) (e.g., Griffis & Stedinger 2007; Rao & Hamed 2000, p. 170) and log-inverse Gaussian (Strupczewski & Kochanek 2009), respectively, save the lower bound parameter. Their variation and asymmetry coefficients depend on two other parameters. The ML estimation procedures for these distributions are the same as the ML procedures for Pearson (3) and inverse Gaussian distributions. However, if a primary PDF, i.e., $f(x)$, is unbounded (see the Gumbel and logistic distributions) and has the only one shape parameter, the resulting PDF, $h(y)$, would possess one shape parameter as well.

The inverse Gaussian distribution represents flood frequency characteristics of Polish rivers quite well (Mitosek *et al.* 2006; Strupczewski *et al.* 2006), in particular of lowland rivers. In fact, the name "inverse Gaussian" is misleading, since it is "inverse" only in that, while the Gaussian describes the distribution of distance at a fixed time in Brownian motion, the inverse Gaussian describes PDF of the first passage time for a Brownian motion starting at zero to reach the absorbing barrier at the fixed point (Cox & Miller 1965, p. 221). The inverse Gaussian distribution arose in

Table 1 | Nonparametric transformations of some soft-tailed distributions

Primary distribution	Probability density function $f(x)$	Transformation	Resulting distribution	Probability density function $h(y)$	The range of the r^{th} moment existence
Normal	$\frac{1}{\sigma\sqrt{2\pi}}\exp\left[\frac{-(x-\mu)^2}{2\sigma^2}\right]$ $\sigma>0;\ -\infty<x<\infty$	$\exp(x)$	Log-normal	$\frac{1}{(y-\epsilon_y)b\sqrt{2\pi}}\exp\left[-\frac{[\ln(y-\epsilon_y)-m]^2}{2b^2}\right]$ $b>0;\ \epsilon_y<y<\infty$	No restriction
Logistic	$\frac{1}{\alpha}\exp\left[-\left(\frac{x-m}{\alpha}\right)\right]\left\{1+\exp\left[-\left(\frac{x-m}{\alpha}\right)\right]\right\}^{-2}$ $\alpha>0;\ -\infty<x<\infty$	$\exp(x)$	Log-logistic	$\frac{1}{\alpha}\left(-\frac{\kappa}{\alpha}y\right)^{1/\kappa-1}\left[1+\left(-\frac{\kappa}{\alpha}y\right)^{1/\kappa}\right]^{-2}$ $\alpha>0,\ \kappa<0;\ 0<y<\infty$	$\kappa\in(-1/r,\ 0)$
			Generalized Log-logistic	$\frac{1}{\alpha}\left(-\frac{\kappa}{\alpha}(y-\epsilon_y)\right)^{1/\kappa-1}\left[1+\left(-\frac{\kappa}{\alpha}(y-\epsilon_y)\right)^{1/\kappa}\right]^{-2}$ $\alpha>0,\ \kappa<0;\ \epsilon_y<y<\infty$	$\kappa\in(-1/r,\ 0)$
Gumbel [*EV1(2)*]	$\frac{1}{\alpha}\exp\{-(x-\xi)/\alpha-\exp[-((x-\xi)/\alpha)]\}$ $\alpha>0;\ -\infty<x<\infty$	$\exp(x)$	Log-Gumbel	$\frac{1}{\alpha}\left(-\frac{\kappa}{\alpha}y\right)^{1/\kappa-1}\exp\left[-\left(-\frac{\kappa}{\alpha}y\right)^{1/\kappa}\right]$ $\alpha>0,\ \kappa<0;\ 0<y<\infty$	$\kappa\in(-1/r,\ 0)$
			Generalized Extreme Value (GEV)	$\frac{1}{\alpha}\left(-\frac{\kappa}{\alpha}(y-\epsilon_y)\right)^{1/\kappa-1}\exp\left[-\left(-\frac{\kappa}{\alpha}(y-\epsilon_y)\right)^{1/\kappa}\right]$ $\alpha>0,\ \kappa<0;\ \epsilon_y<y<\infty$	$\kappa\in(-1/r,\ 0)$
Exponential	$\beta\exp[-\beta(x-\epsilon_x)]$ $\beta>0;\ \epsilon_x<x<\infty$	$\exp(x)$	Pareto	$\frac{\beta}{\epsilon_y}\left(\frac{y}{\epsilon_y}\right)^{-(\beta+1)};\ \beta>0;\ \epsilon_y<y<\infty,\ \epsilon_y=\exp(\epsilon_x)$	$\beta>r$
			Generalized Pareto	$\frac{1}{\alpha}\left[1-\frac{\kappa}{\alpha}(y-\epsilon_y)\right]^{1/\kappa-1}$ $\alpha>0,\ \kappa<0;\ \epsilon_y<y<\infty,\ \epsilon_y=\exp(\epsilon_x),\ \alpha\neq\epsilon_y/\beta,$ $1/\kappa=-\beta$	$\kappa\in(-1/r,\ 0)$
Pearson (3)	$\frac{\alpha^\lambda}{\Gamma(\lambda)}(x-\epsilon_x)^{\lambda-1}\exp[-\alpha(x-\epsilon_x)]$ $\alpha,\ \lambda>0;\ \epsilon_x<x<\infty$	$\exp(x)$	Log-Pearson (3)	$\frac{\alpha^\lambda}{y\Gamma(\lambda)}[\ln(y/\epsilon_y)]^{\lambda-1}\exp[-\alpha\ln(y/\epsilon_y)]$ $\alpha>0,\ \lambda>1;\ 0<\epsilon_y<y<\infty$	$\alpha\geq r$
		$(x-\epsilon_x)^{-1}$	Inverse Pearson (3)	$\frac{\alpha^{-(m+1)}}{\Gamma[-(m+1)]}(y-\epsilon_y)^m\exp[-\alpha/(y-\epsilon_y)]$ $\alpha>0,\ m<-1;\ \epsilon_y<y<\infty$	$m<-(r+1)$

Table 1 | *(continued)*

Inverse Gaussian	$\dfrac{\alpha}{\sqrt{\pi}\sqrt{(x-\epsilon_x)^3}}\exp\left[-\dfrac{\left(\alpha-\frac{\beta}{\alpha}(x-\epsilon_x)\right)^2}{(x-\epsilon_x)}\right]$	$\exp(x)$	Log-Inverse Gaussian	$\dfrac{\alpha}{\sqrt{\pi}y\left[\ln(y/\epsilon_y)\right]^{3/2}}\exp\left[-\dfrac{\left(\alpha-\frac{\beta}{\alpha}\ln(y/\epsilon_y)\right)^2}{\ln(y/\epsilon_y)}\right]$	$\frac{\beta}{\alpha}>\sqrt{r}$
	$\alpha,\ \beta>0;\ \epsilon_x<x<\infty$	$(x-\epsilon_x)^{-1}$	Inverse of Inverse Gaussian	$\dfrac{\alpha}{\sqrt{\pi(y-\epsilon_y)}}\exp\left[-\dfrac{[\beta-\alpha^2(y-\epsilon_y)]^2}{\alpha^2(y-\epsilon_y)}\right]$	No restriction
				$\alpha,\ \beta>0;\ \epsilon_y<y<\infty$	

flood routing modelling (Hayami 1951; Dooge 1973) under the name "convective diffusion" (*CD*) model as the impulse response of the linear channel at a fixed distance for the Froude number equal to zero and applied in FFA as a PDF by Strupczewski *et al.* (2001*b*, 2002*b*, 2003). The similarity between the convective diffusion (*CD*) and the log-normal (*LN*) distributions and related model discrimination problems were investigated by Strupczewski *et al.* (2003).

Taking into account the interest in flood frequency analysis in the right tail estimation and the doctrine of parameter parsimony, a replacement of the lower bound parameter by the second shape parameter seems to be advisable. The background and arguments for adding the second shape parameter as a replacement of the lower bound parameter are discussed by Strupczewski *et al.* (2008). Let $f(x;\ \alpha,\ \beta)$ be the PDF of a variable with lower bound at zero, where α and β are the scale and shape parameters. In principle there are three ways of introducing the second shape parameter, i.e., the power transformation of the variable (*Tx*), its density function (*Tf*) and/or its cumulative distribution function (*TF*). None of them changes the variability range, i.e., $0\le x\le\infty$.

Tx. Transformation of the variable by putting $x=y^n$. Then the PDF of y is

$$h(y;\alpha,\beta,n)=|n|y^{n-1}f(x;\alpha,\beta) \tag{1}$$

and quantiles are related by

$$y(H)=\begin{cases}[x(H=F)]^{\frac{1}{n}} & \text{for } n>0\\ [x(H=1-F)]^{\frac{1}{n}} & \text{for } n<0.\end{cases} \tag{2}$$

Tf. Density transformation by raising $f(x;\ \alpha,\ \beta)$ to the power

$$h(x;\alpha,\beta,n)=[f(x;\alpha,\beta)]^n/\int_0^\infty[f(x;\alpha,\beta)]^n dx \quad \text{for } n>0. \tag{3}$$

TF. Power transformation of the cumulative distribution function $F(x;\ \alpha,\ \beta)$

$$H(x;\alpha,\beta,n)=[F(x;\alpha,\beta)]^n \tag{4}$$

to have $H=(x=0;\ \alpha,\ \beta,\ n)=0$ and $H=(x=\infty;\ \alpha,\ \beta,\ n)=1$, exponent n should be positive real value. Then the PDF is

$$h(x;\alpha,\beta,n)=n[F(x;\alpha,\beta)]^{n-1}f(x;\alpha,\beta);\quad n>0. \tag{5}$$

Note that the PDF (Equation (5)) can be explicitly analytically defined if the $F(x)$ has a closed form.

Not all of the three ways of introducing the second shape parameter are feasible for every distribution. In some cases the transformation does not yield the second shape parameter, i.e., after conversion of transformed PDF one gets the initial distribution function; in other cases the transformation is cumbersome. However, it is interesting that regardless of the method of transformation, some of the two-shape-parameter distributions are heavy-tailed for a certain combination of shape parameters (Table 2). Let us take gamma *Tx* distribution as an example. With positive values of shape parameters it was introduced to FFA by Krickiy & Menkel (1950) and for the first time published in 1946, known under the name "Krickiy and Menkel distribution". It is a light-tailed distribution which for the value of the shape parameter n (see Equation (1)) going to zero becomes a heavy-tailed-like distribution. Quantiles were estimated by the tables for the given probability of exceedance ($\overline{F}$), the coefficient of variation (C_V) and the ratio of skewness to variation (C_S/C_V). To set up the tables, Krickiy & Menkel (1950) must have solved repeatedly the set of the complicated systems of non-linear equations and they managed to do so before computers became available. With negative values of shape parameters, the gamma *Tx* distribution has a heavy tail (Strupczewski 1964; Strupczewski *et al.* 2008). The same transformation applied to the inverse Gaussian variable (Table 2) gives soft-tailed distribution both for positive and negative value of the shape parameter n and it becomes an inverse-power-like distribution for $n\to 0$. The use of the density transformation (*Tf*) for the inverse Gaussian PDF provides a soft-tailed distribution (Strupczewski *et al.* 2008) recognized as the Halphen type A distribution (Perreault *et al.* 1999), which is found to be an excellent candidate for frequency analysis of extremes.

There are only a few heavy-tailed distributions from those listed in Tables 1 and 2 which are commonly used in FFA. The Flood Estimation Handbook (FEH) (Robson & Reed 1999) recommends adoption of the GLL distribution together with Linear moments (LMM) as the parameter estimation method for annual peak flows in the UK, while prior to the publication of the FEH, the distribution most widely used in the UK was GEV (NERC 1975). The log-Pearson (3) distribution is the default distribution for flood frequency analysis in the United States (US Water Resources Council 1982; Griffis & Stedinger 2007; Stedinger & Griffis 2008) and in Australia. The general Pareto is in common use for modelling the distribution of excess over threshold or Peak Over Threshold method (e.g., Leadbetter *et al.* 1983; Van Monfort & Witter 1986; Rosbjerg *et al.* 1992; Madsen *et al.* 1997).

MODEL SELECTION

Makkonen (2008) noted that the belief in the applicability of the extreme value theory is so strong that the analysis is commonly done, even when a good fit should not be expected due to the asymptotic nature of the theory. The selection of a correct or best-fitting distribution can have a significant effect on the reliability of flood-related structures. Even if the sample size is not sufficiently large for making a correct selection with a high probability, a method of selection is still required and whatever information is available it needs to be utilized. In general, even though two models may exhibit similar fits to given data, it is, nonetheless, desirable for FFA to select the true (or "more correct") model, since inferences based on the model will involve tail probabilities where the effect of the model selection is more pronounced and critical.

The classical approach to model selection employs either of two statistical identification approaches as a decision procedure for statistical model building or identification: (1) goodness-of-fit procedure which is of little value for model selection in hydrology or (2) discrimination procedure. Both approaches, by definition, take into account the whole range of data in the sample. The discrimination procedures that are commonly used in hydrology define a test statistic as well as a decision rule indicating the action to be taken for each observed sample. Having defined the discrimination procedure, one selects from a set of competing models the model that is, according to the decision rule, best fitted to the data.

Table 2 | Two-shape parameter heavy-tailed distribution functions got by parametric transformations

Primary distribution	Probability density function $f(x)$	Transformation	Probability density function $h(y)$	The range of the r^{th} moment existence
Weibull	$\frac{\kappa}{\alpha}\left(\frac{x}{\alpha}\right)^{\kappa-1}\exp\left[-\left(\frac{x}{\alpha}\right)^{\kappa}\right]$ $\alpha,\ \kappa>0;\ x>0$	Tf	$\frac{\kappa\cdot n^{\frac{1+n(\kappa-1)}{\kappa}}}{\alpha\Gamma\left[\frac{1+n(\kappa-1)}{\kappa}\right]}\left(\frac{y}{\alpha}\right)^{n(\kappa-1)}\exp\left[-n\left(\frac{y}{\alpha}\right)^{\kappa}\right]$ $\alpha,\ \kappa,\ n>0;\ y>0$	$r>-[1+(\kappa-1)\cdot n]$
Gamma	$\frac{\alpha^{\lambda}}{\Gamma(\lambda)}(x)^{\lambda-1}\exp[-\alpha\cdot x]$ $\alpha,\ \lambda>0;\ x>0$	Tx	$\frac{\lvert n\rvert\alpha^{(m+1)/n}}{\Gamma[(m+1)/n]}y^{m}\exp[-\alpha\cdot y^{n}]$ $\alpha,\ m,\ n>0$ and $m<-1$ for $n<0;\ y>0$	$r<-(m+1)$ for $n<0$ and $m>0,\ n>0$
Inverse Gaussian	$\frac{\alpha}{\sqrt{\pi}\sqrt{x^3}}\exp\left[-\frac{\left(\alpha-\frac{\beta}{\alpha}x\right)^2}{x}\right]$ $\alpha,\ \beta>0;\ x>0$	Tx	$\frac{\lvert n\rvert\cdot\alpha}{\sqrt{\pi\cdot y^{n+2}}}\exp\left[-\left(\alpha-\frac{\beta}{\alpha}y^{n}\right)^2/y^{n}\right]$ $\alpha,\ \beta>0;\ y>0$	No restrictions
		$Tf^{(*)}$	$\frac{\alpha^{3n-2}\exp(-2n\beta)}{2\beta^{3n/2-1}K_{\frac{3n}{2}}(2n\beta)}y^{-3n/2}\exp\left[-\frac{n}{y}\left(\alpha-\frac{\beta\cdot y}{\alpha}\right)^2\right]$ $\alpha,\ \beta,\ n>0;\ y>0$	No restrictions
Log-logistic	$\frac{1}{\alpha}\left[-\frac{\kappa}{\alpha}x\right]^{1/\kappa-1}\left[1+\left\{-\frac{\kappa}{\alpha}x\right\}^{1/\kappa}\right]^{-2}$ $\alpha>0,\ \kappa<0;\ x>0$	TF	$\frac{n}{\alpha}\left[-\frac{\kappa}{\alpha}y\right]^{1/\kappa-1}\left[1+\left\{-\frac{\kappa}{\alpha}y\right\}^{1/\kappa}\right]^{-(n+1)}$ $\alpha,\ n>0,\ \kappa<0;\ y>0$	$\kappa\in(-\frac{1}{r},0)$
		Tf	$\frac{1}{\alpha}\frac{\Gamma(2n)}{\Gamma[n(1+\kappa)-\kappa]\cdot\Gamma[n(1-\kappa)+\kappa]}\left(-\frac{\kappa\cdot y}{\alpha}\right)^{n(1/\kappa-1)}\left[1+\left(-\frac{\kappa\cdot y}{\alpha}\right)^{1/\kappa}\right]^{-2n}$ $\alpha,\ n>0,\ \kappa<0,\ \frac{n}{\kappa}+n<1<-\frac{n}{\kappa}+n;\ y>0$	$n/\kappa+n-1<r<-n/\kappa+n-1$
Log-Gumbel	$\frac{1}{\alpha}\left(-\frac{\kappa}{\alpha}y\right)^{1/\kappa-1}\exp\left[-\left(-\frac{\kappa}{\alpha}y\right)^{1/\kappa}\right]$ $\alpha>0,\ \kappa<0;\ x>0$	Tf	$\frac{1}{\alpha}\frac{n^{\kappa+n-n\kappa}}{\Gamma[n(1-\kappa)+\kappa]}\left(-\frac{\kappa\cdot y}{\alpha}\right)^{n(1/\kappa-1)}\exp\left[-n\left(-\frac{\kappa\cdot y}{\alpha}\right)^{1/\kappa}\right]$ $\alpha,\ n>0,\ \kappa<0,\ -n/\kappa+n>1;\ y>0$	$r<-n/\kappa+n-1$
Pareto	$\frac{1}{\alpha}\left(1-\frac{\kappa}{\alpha}x\right)^{1/\kappa-1}$ $\alpha>0,\ \kappa<0;\ x>0$	Tx	$\frac{\lvert n\rvert}{\alpha}y^{n-1}\left(1-\frac{\kappa\cdot y^{n}}{\alpha}\right)^{1/\kappa-1}$ $\alpha>0,\ \kappa<0;\ y>0$	$r<-n/\kappa$ for $n>0$ and $r<-n$ for $n<0$

(*)Substituting $n\beta=\mathfrak{z},\ n=\frac{2}{3}(1-\mathfrak{I}),\ \alpha^2/\beta=m$ one obtains the Halphen type A distribution (Perreault *et al.* 1999).

Mitosek *et al.* (2006) analysed the efficiency of three discrimination procedures, i.e., the maximized logarithm of the likelihood function (K), the density function of the scale transformation maximal invariant (QK) and the difference between maximum likelihood method and method of moment estimates of 1% quantile (R) and then fit four two-parameter distribution functions (*Ga*, *LN*, *We*, *CD*) to 39 historical time series of Polish data. Introductory studies on the efficiency of these discrimination procedures as well as further studies of Strupczewski *et al.* (2006) show that in the ideal case, i.e., if the competitive set of models contains the true PDF, the probabilities of correct selection are probably unacceptable for "hydrological" sample sizes, and samples of sizes $N \geq 100$ are usually required to give large levels for the probabilities of correct selection. The discrimination power decreases sharply with the number of competitive models. In reality, one deals with the hypothetical PDF (H), called here the false distribution function (F), which differs more or less from the true one. This produces a model error in any statistical characteristic of the distribution. Its magnitude for a given characteristic depends not only on how close F is to T but on the estimation method as well.

As far as the Polish gauging stations were concerned, the studies revealed that the *CD* model has been selected as the best by the K and R procedures, whilst the QK procedures pointed to the *LN* model. As one can see, depending on the discrimination procedure applied, Polish datasets can be either *CD* or *LN*. Such contradictory results mean that one has to look for the ways to increase the efficiency of the model selection by, e.g., using several discrimination procedures (for the same datasets and models), combined with the knowledge of their efficiency for a given case supplemented by the classical graphical analysis on the probability paper.

Recently, catering for the extreme value theory and accepting the fact that none of simple parametric models can fit data equally well in their whole range, the balance in quantile estimation and distribution fitting has drifted towards the methods which attach greater weight to the tails of distributions and hence to largest elements in the sample rather than to the whole range of data. This approach is a consequence of the belief that the key information for FFA purposes, i.e. the upper quantiles, can be "read" from the tail of distributions based on the largest elements in the sample regardless of their, usually very poor, quality. Therefore, the estimation of tail behaviour may be a fundamentally different problem than that of estimating a suitable density function for the main body of the data.

Moon & Lall (1994) considered two types of methods for tail estimation. The first method is the use of nonparametric approach by estimating kernel quantile based on full sample and extrapolating the empirical quantile through the use of boundary kernels. The second type focuses on the k upper elements of the sample and seeks to develop parametric form for the tail only. The quadratic tail model that is quadratic in $\ln \overline{F}$ proved to be the best in terms of bias, RMSE and robustness for a variety of situations tested. Wang (1997), on the other hand, introduced LH moments (a generalization of "classical" linear moments) which are based on a linear combination of higher-order statistics and as such deal with the upper part of the distribution and the largest elements in the sample.

Following the concept of concentrating on the (heavy) tails of distributions El Adlouni *et al.* (2008) proposed a useful and practical two-step procedure of model selection: (1) to identify which class of the distributions (heavy- or light-tailed) the analysed dataset belongs to, and (2) to use classical criteria and tests for model selection within the pointed class. The distribution functions, commonly used in hydrology, are divided according to the thickness of the tail into five classes: A (for the heaviest) to E (the lightest). The set of tests which helps with the distribution of the dataset into a certain class has been implemented in HYFRAN Plus software (El Adlouni *et al.* 2008). It is recommended to start testing with the log–log plot, which may allocate datasets into class C regularly varying distributions, i.e. Fréchet (*EV2*), Halphen IB (*HIB*), Log-Pearson 3 (*LP3*), Inverse Gamma (*IG*), or suggests further testing.

The log–log test called, also tail probability plot, consists in the fact that for the exponential tail with mean μ:

$$\overline{F}(u) = P(X > u) = \exp(-u/\mu) \tag{6}$$

and for power-law large quantiles

$$\overline{F}(u) = P(X > u) \approx C \int_u^{\infty} \frac{1}{x^{\alpha}} dx = C \frac{1}{\alpha - 1} u^{1-\alpha} \tag{7}$$

$\alpha > 1$ is the tail index (the smaller the α, the more heavy-tailed the distribution). Taking the logarithm of (6) and (7) one obtains

$\ln[P(X>u)] \approx -u/\mu$ and $\ln[P(X>u)] \approx \ln[C/(\alpha-1)] + (1-\alpha)\ln(u)$, respectively, i.e. formula of straight lines.

Consequently, supposing that particular dataset points, in their whole range, form a more or less straight line on the log–log plot, it means that the data reflect the pattern of Pareto-type distribution (B class). Such a situation of good fitting to all elements of dataset, however, hardly happens in reality, and usually only upper part of the data (if at all) follows the straight line. One can assume, that when the largest elements in a sample fall into the line, the dataset is most probably heavy-tailed narrowing down the range of models to a few competing hydrological distributions only. If the log–log test fails, i.e., the data do not belong to the C class, HYFRAN suggests Mean Excess Function test which enables data allocation to class D or E which, as representing light-tailed distributions, are of minor interest here. Once the class of the distributions is approved, the selection of an appropriate distribution from among the competitors within the class can be continued by means of classical tests and criteria, such as Akaike Information Criterion (AIC) (Akaike 1970; Hurvich & Tsai 1989) or Bayesian Information Criterion (BIC) (Schwarz 1978). The results of the application of this procedure to the Polish annual peak-flood datasets will be described in detail in the penultimate section.

MODEL ERROR

In practice one deals with "false" model and is not able to assess the magnitude of model error of any estimated statistics. To that end, the "true" PDF together with its parameter values should be known. The model bias of large quantile estimates depends on both the estimation method and sample size. The interest is to find a most robust estimation method for large quantiles under the false distribution assumption. Strupczewski *et al.* (2002*a*, *c*) analytically evaluated an asymptotic bias of four estimation methods caused by the assumption of a false probability distribution. The estimation methods were used by approximating the "true" model by the "false" one. Let us take, for example, the two bounded at zero two-parameter PDFs, i.e., the "true" $f^{(T)}(x;\ \theta_1{}^{(T)},\ \theta_2{}^{(T)})$ and the "false" one $f^{(F)}(x;\ \theta_1{}^{(F)},\ \theta_2{}^{(F)})$. The method of moments (MOM), used as an approximation method, reduces to the moment matching of F to T distribution:

$$\int_0^\infty x^r f^{(F)}(x;\theta_1^{(F)},\theta_2^{(F)})dx = \int_0^\infty x^r f^{(T)}(x;\theta_1^{(T)},\theta_2^{(T)})dx \quad \text{for } r=1,2 \tag{8}$$

Similarly, LMM, as an approximation method, reduces to the L-moment or probability weighted moment matching:

$$\int_0^\infty x\cdot[F^{(F)}(x;\theta_1^{(F)},\theta_2^{(F)})]^{r-1} f^{(F)}(x;\theta_1^{(F)},\theta_2^{(F)})dx = \int_0^\infty x\cdot[F^{(T)}(x;\theta_1^{(T)},\theta_2^{(T)})]^{r-1} f^{(T)}(x;\theta_1^{(T)},\theta_2^{(T)})dx \quad \text{for } r=1,2 \tag{9a}$$

or equivalently

$$\int_0^1 x(F^{(F)};\theta_1^{(F)},\theta_2^{(F)})[F^{(F)}]^{r-1}dF^{(F)} = \int_0^1 x(F^{(T)};\theta_1^{(T)},\theta_2^{(T)})[F^{(T)}]^{r-1}dF^{(T)} \quad \text{for } r=1,2 \tag{9b}$$

where $F^{(\cdot)}$ is the cumulative probability distribution.

In order to apply the Maximum Likelihood Method (MLM) as an approximation method of one distribution (T) by another (F), one has to consider the asymptotic sample of T-distribution. Then, the ML equations have the form:

$$\lim_{N\to\infty} \mathrm{E}\left(\frac{\partial \log L_N^{(F)}(x;\theta_1^{(F)},\theta_2^{(F)}|T)}{\partial\theta_r^{(F)}}\right) = \int_0^\infty \frac{\partial \log f^{(F)}(x;\theta_1^{(F)},\theta_2^{(F)})}{\partial\theta_r^{(F)}} f^{(T)}(x;\theta_1^{(T)},\theta_2^{(T)})dx = 0 \quad r=1,2 \tag{10}$$

where $\log L^{(F)}$ denotes the log-likelihood function for the false distribution.

In order to derive the asymptotic bias (B) of a quantile x_p caused by the false (F) choice of the distributional hypothesis (H), the knowledge of the true distribution (T) together with the value of its parameters is necessary. Then, the problem is defined as an approximation of the T-function by the F-function and it, therefore, remains no longer a statistical estimation problem. Having approximated T by F, one can

find for any quantile x_p, where p is the probability of exceedance ($p \equiv \overline{F}$), both the value of x_p of the approximated function, i.e. $x_p^{(T)}$, and the corresponding value of x_p of the approximating function, i.e. $x_p^{(F)}$. Thus, the asymptotic relative bias of a quantile, x_p, is defined as

$$RB(x_p) = (x_p^{(F)} - x_p^{(T)})/x_p^{(T)}.$$

Several pairs of two-parameter distributions bounded at zero showed that the asymptotic bias of large quantiles is an increasing function of the true value of the coefficient of variation (C_V), being smallest for the MOM and largest for MLM. The bias of LMM occupied an intermediate position. Figure 1 shows the asymptotic relative bias of quantiles if the log-normal distribution asymptotic sample was falsely recognized as the log-Gumbel distributed. This finding essentially diminishes the practical usefulness of MLM in hydrological extremes analysis, because its efficiency may not compensate for the (frequently) huge bias produced by the assumption of a false PDF in the region of small exceedance probability quantiles the user is often interested in. It marks a departure of hydrological extreme value analysis from classical statistical theory of extremes whose core is the maximum likelihood method.

As shown in Figure 1, the upper quantile estimates obtained by the *L*-moment matching are much less sensitive to the false distribution choice than are the ML estimates. Computational simplicity, small biases of sample estimates of *L*-moments and applicability for heavy-tailed distributions (namely, *L*-moments exist whenever the mean of the distribution exists) give preference to the *L*-moment method in FFA (Hosking & Wallis 1997).

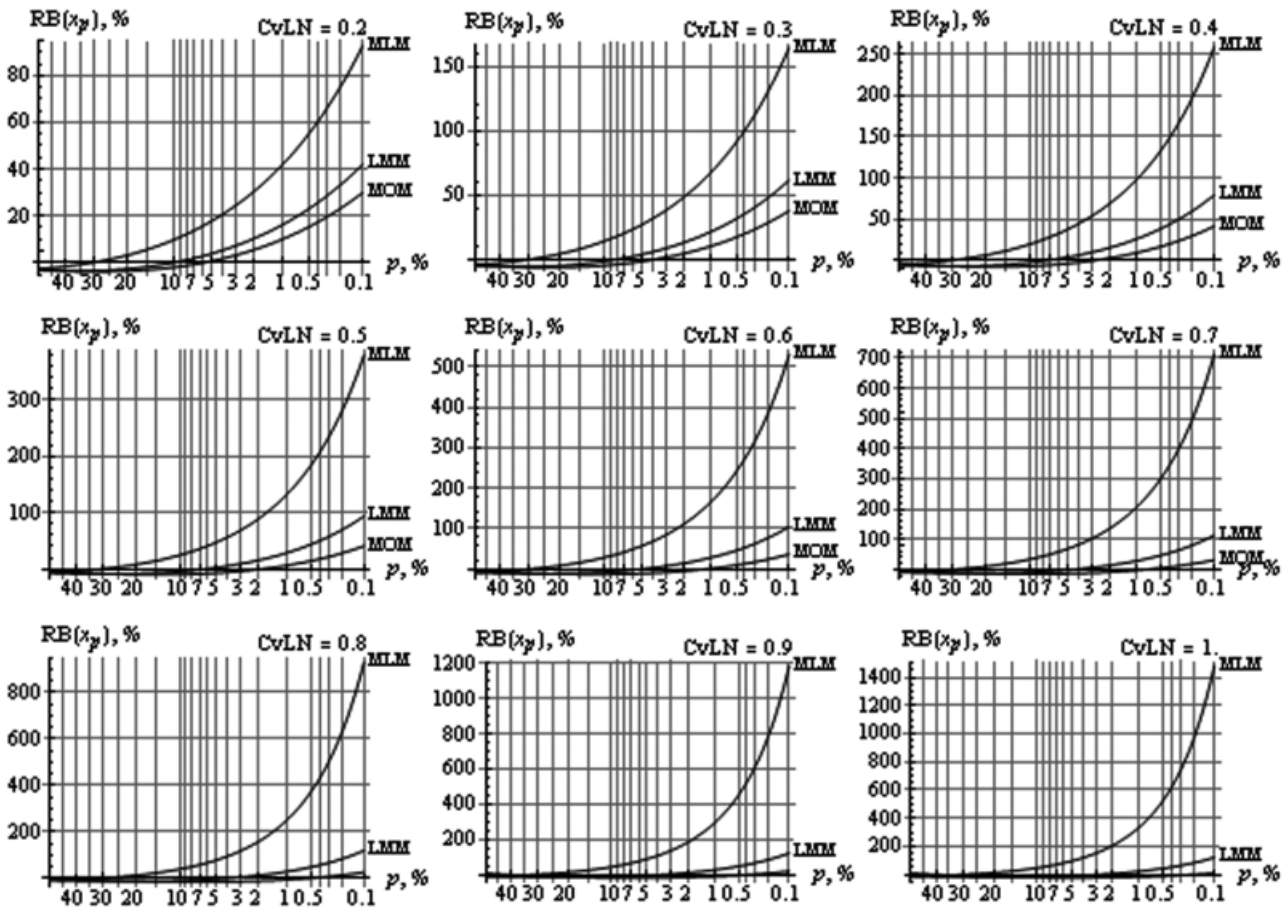

Figure 1 | Asymptotic bias of *LG* quantiles vs. probability of exceedance for some selected values of the true coefficient of variation $C_V LN$.

In fact, moment estimators have some undesirable properties. Wallis *et al*. (1974) assessed the dependence of the bias of sample standard deviation (*SD*) and skewness (C_S) on the distribution function, population skewness and sample size. Bias of both *SD* and C_S is negative and its absolute value grows with an increase of C_S, tending to zero with a sample size. Its algebraic bounds depend on the sample size. The algebraic bounds of skewness and kurtosis discovered for mathematical statistics by Wilkins (1944) and for hydrology by Kirby (1974) are recognized in hydrology (e.g., Hosking & Wallis 1997). Extending the Wallis *et al*. (1974) assessment for heavy-tailed distributions, we have found by simulation experiments that for two-parameter distributions bounded at zero, the sampling coefficient of variation C_V is heavily underestimated and moreover the negative bias remains considerably high even for statistical large samples. It is shown for the log-Gumbel distribution in Figure 2. As one can see, for the population coefficient of variation $C_V = 2$ and sample size $N = 10{,}000$, the average sampling $\hat{C}_V$ equals 1.47, which gives the bias of −26%. Such high underestimation cannot be solely explained by the algebraic bound of C_V (Katsnelson & Kotz 1957). Note that the algebraic bound depends on the sample size but not on the distribution and its population value of C_V. For a set of N non-negative values x_i, not all equal, the coefficient of variation $\hat{C}_V$ cannot exceed $(N-1)^{1/2}$, attaining this value if and only if all but one of the x_i are zero. Hence, for $N = 10{,}000$ one gets the upper bound max $\hat{C}_V \approx 100$, while the largest population C_V considered equals two.

Note that the sampling moments are always finite, i.e., even if the respective population moments do not exist. Therefore, to be strict, allowance for heavy-tailed distributed samples ceases to apply MOM unless one takes for granted that the population values of the matched moments are finite. In fact, it is not easy to accept for hydrologists with civil engineering background that the inertia centre or inertia moment of a figure may be undefined, while quantiles are still finite values. The same dilemma appears in non-stationary parametric approach to FFA (Strupczewski & Kaczmarek 2001; Strupczewski *et al*. 2001*a*, 2009; Sankarasubramanian & Lall 2003; Khaliq *et al*. 2006). To bring closer together FFA in changing environment and trends in climatological time series investigations, and to get results of different distributions comparable, the time-trend is assumed in the first moments of a distribution. Therefore, apart from the estimation technique one should take for granted that these time-dependent moments in populations are finite.

Evaluating the asymptotic bias of upper quantiles caused by the false distributional assumption, one should expect that for a finite sample the bias would likely be a little greater. It is so because even for the correct distributional assumption, any estimation method is not bias free for small samples. However, sometimes the model bias and estimation bias may be of opposite sign. Moreover, for some pairs (F; T) such tendency may be counter-balanced by the influence of the sample range, which grows with its size and to which false distribution function is fitted.

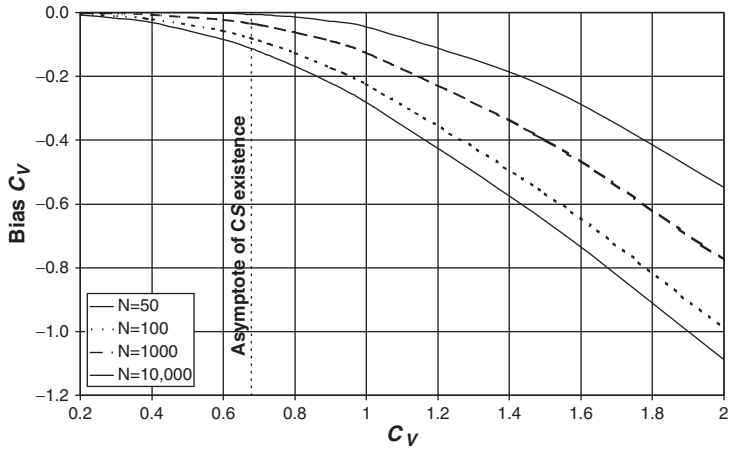

Figure 2 | Bias of MOM estimate of the variation coefficient C_V for Log-Gumbel samples of various sizes (N).

To study the sampling properties of the bias we performed simulation experiments on several (F; T) pairs. The results of ($F=LG$, $T=LN$) and ($T=LN$) are presented in Table 3. The relative bias (δB) and relative root mean square error ($\delta RMSE$) of $\hat{x}_{F=.99}$ for three estimation methods, three values of the coefficient of variation of the "true" distribution, i.e. $C_V^{(LN)}$, and various sample sizes, including asymptotic sample, are shown in Table 3. As one can see, MOM for ($F=LG$, $T=LN$) happens to be superior both in terms of bias and MSE for any sample size. MLM gives the greatest bias and MSE of the three estimation methods. The sampling bias of $x_{1\%}$ for ($F=LG$, $T=LN$) is slowly increasing with the sample size for the ML-method. It points to different signs of the two components, i.e., of model and estimation biases. For MOM and $C_V^{(LN)}=1.0$ is just the opposite tendency as the both components are negative values. A slight variability of the bias with a sample size observed for all methods indicates a prevailing share of the model bias in the sampling bias value. The high magnitude of MLM relative bias for ($F=LG$, $T=LN$) is striking. Even for very small samples the bias of MLM for ($F=LG$, $T=LN$) is much greater than for the two other methods and at least one order greater than for ($T=LN$). For $C_V^{(LN)}=1.0$ and $N=60$ it equals 324.8% and −0.306% for ($F=LG$, $T=LN$) and ($T=LN$), respectively. Note the substantial discrepancies in results between ($F=LG$, $T=LN$) and ($T=LN$) cases. MOM gives the greatest bias of the three estimation methods for ($T=LN$) and the smallest one for ($F=LG$, $T=LN$). In particular the results for MOM with $C_V^{(LN)}\geq 0.6$ are worthy of attention. While the biases of $x_{F=0.99}$ for ($F=LG$, $T=LN$) and ($T=LN$) are of similar magnitude, the MSE value is even lower for wrong distributional assumption, i.e., for (H = LG).

Aimed as a continuation of pioneering studies by Landwehr *et al.* (1980) and Kuczera (1982) using simulation techniques, Kochanek *et al.* (2005) assessed the performance of various models combined with three estimation methods, i.e., MOM, LMM and MLM, versus five five-parameter specific Wakeby distributions serving as flood parent distributions. The MLM was found to produce usually the largest values of both bias and RMSE of upper quantiles for hydrological (i.e., up to 100 elements) sample sizes. Moreover, some calculations of three-parameter distributions estimated by MLM in many cases did not give the 100% reliability even for a large sample size; the procedure for *GEV* performed particularly badly. The results of Kochanek *et al.* (2005), however, deal with the case when the parent distribution is known and so are the errors resulting from wrong decisions as to the model choice. In reality, the situation is more

Table 3 | Relative bias (δB) and the relative root mean square error ($\delta RMSE$) of $x_{F=0.99}$ (%) for the log-normal distributed samples assuming Log-Gumbel and Log-normal function

		$F=LG$, $T=LN$						$T=LN$					
		MOM		LMM		MLM		MOM		LMM		MLM	
$C_V^{(LN)}$	N	δB	$\delta RMSE$	δB	$\delta RMSE$	δB	$\delta RMSE$	δB	$\delta RMSE$	δB	$\delta RMSE$	δB	$\delta RMSE$
0.2	20	8.065	12.83	16.59	20.67	33.99	40.44	−1.574	8.691	0.191	8.875	−1.416	8.634
	60	9.399	11.10	16.39	16.39	38.61	41.20	−0.531	5.089	0.061	5.049	−0.451	4.984
	100	9.662	10.71	16.34	16.34	39.83	41.46	−0.327	3.963	0.023	3.901	−0.322	4.070
	∞	10.08	10.00	16.31	16.31	42.09	42.09	0	0	0	0	0	0
0.6	20	−3.006	21.21	29.91	45.02	142.6	190.5	−5.500	25.79	1.189	26.51	−2.087	23.98
	60	0.169	13.26	29.45	35.24	156.4	174.9	−2.087	16.40	0.386	14.97	−0.674	13.84
	100	0.924	10.68	29.33	32.94	160.2	171.9	−1.271	13.21	0.209	11.56	−0.449	10.70
	∞	2.194	2.194	29.22	29.22	167.4	167.4	0	0	0	0	0	0
1.0	20	−21.69	32.26	23.13	49.25	312.7	490.3	−11.41	38.64	2.097	43.30	−0.999	37.17
	60	−18.18	23.73	23.67	35.06	324.8	385.9	−5.319	26.38	0.723	24.33	−0.306	21.01
	100	−17.19	21.19	23.76	31.22	328.9	366.5	−3.524	22.14	0.442	18.82	−0.245	16.16
	∞	−15.04	15.04	23.90	23.90	337.9	337.9	0	0	0	0	0	0

complex, because the real distribution is not known and it is practically impossible to calculate and then compare any false-model-choice errors or efficiency of a particular "distribution/estimation method" procedure.

UPPER QUANTILES OF VARIOUS DISTRIBUTIONS

A number of investigators have argued in favour of the applicability of inverse power-low statistics to floods. Leaving the evidence for heavy tails of hydrologic extremes aside and the question whether an inverse power-law estimate of the flood hazard is preferable to other statistical distributions, one should evaluate the practical importance of the problem, i.e., what consequences in terms of hydraulic design values stem from the replacement of thin-tailed distributions by heavy-tailed distributions. Heavy-tailed distribution quantiles are considered to provide higher flood frequency estimates than thin-tailed probability distributions, even if they have the same statistical characteristics (mean and variance) especially for a large non-exceedance probability (e.g., Malamud & Turcotte 2006; El Adlouni *et al*. 2008).

Our objective here is to compare the upper quantile values of various heavy- and soft-tailed distributions with the same summary statistics values used for distribution fitting. In this respect, the moment and *L*-moment summary statistics are employed for the sets of two- and three-parameter distributions with different values of the coefficients of variation C_V and L-C_V, and the coefficients of skewness C_S and L-C_S, respectively.

To compare quantile values got by the *L*-moment matching, the *L*-moments must be derived for each distribution considered. To obtain them, the explicit analytical form of the cumulative distribution function $F(x)$ or the quantile function x_F must exist as the *L*-moments of the probability distribution are defined by (e.g. Hosking & Wallis 1997):

$$\lambda_r = \int_0^1 x(F)\cdot\phi_r(F)dF \equiv \int_{-\infty}^{+\infty} x\cdot\phi_r[F(x)]\cdot f(x)dx \quad \text{where } r = 1, 2, \ldots \tag{11}$$

However, it is not always the case. This obstacle can be easily overcome by numerical integration using, e.g., algorithms built in the Wolfram Mathematica package. It has enabled us to include the two- and three-parameter inverse Gaussian distribution into our comparison. The simulation approach has been proposed as an alternative and for checking numerical results (Markiewicz & Strupczewski 2008). Note that the *L*-moments ratio estimates have very small biases even in moderate samples (Hosking & Wallis 1997, p. 28). Hence, generating a long sequence one can get the relationships between the distribution parameters and the *L*-moments and their ratios.

Results obtained for the *L*-moment matching for both two-parameter distributions (Table 4) and three-parameter distributions (Table 5) are in full agreement with the common conviction that the upper quantiles of heavy-tailed distributions provide higher values of upper quantiles than those of other distributions. For two-parameter distributions (Table 4),

Table 4 | Upper quantiles vs. the coefficient of *L*-variation. Two-parameter distributions and the *L*-moments method, while the first *L*-moment: $\lambda_1 = 100$

		$x_{F=0.99}$				$x_{F=0.999}$			
PDF	**L-C_V (τ)**	**0.1**	**0.2**	**0.3**	**0.35**	**0.1**	**0.2**	**0.3**	**0.35**
Log-Gumbel		160.93	270.70	395.00	467.14	206.43	497.78	944.83	1269.22
Log-Logistic		157.45	236.31	341.21	405.80	199.57	376.91	683.32	913.08
Log-normal		149.10	215.79	307.12	360.46	170.89	283.70	466.25	587.24
Inverse Gaussian		151.20	214.35	301.46	355.00	172.69	276.23	432.69	535.86
Gumbel		159.60	216.06	275.65	303.88	193.78	282.61	376.39	420.81
Gamma		146.57	202.14	269.76	308.72	164.95	248.65	357.04	422.11
Weibull		135.77	182.10	248.86	289.75	144.51	207.30	307.08	373.34
Normal		141.87	183.75	223.30	244.23	155.62	211.25	263.78	291.59

Table 5 | Upper quantiles vs. the coefficient of *L*-skewness. Three-parameter distributions and *L*-moments method, while the first *L*-moment: $\lambda_1 = 0$ and the second *L*-moment $\lambda_2 = 1.0$

		$x_{F=0.99}$					$x_{F=0.999}$				
PDF	***L*-C$_S$ (τ_3)**	**0.17**	**0.2**	**0.25**	**0.3**	**0.33**	**0.17**	**0.2**	**0.25**	**0.3**	**0.33**
GEV		5.804	6.213	6.935	7.699	8.171	9.131	10.374	12.860	15.956	18.144
GLL		6.362	6.726	7.360	8.023	8.432	12.253	13.618	16.246	19.388	21.548
Log-normal		5.746	6.094	6.717	7.397	7.833	9.075	9.969	11.684	13.737	15.160
Inverse Gaussian		5.675	5.994	6.562	7.184	7.586	8.718	9.429	10.731	12.206	13.191
Pearson (3)		5.575	5.854	6.336	6.849	7.173	8.383	8.958	9.962	11.043	11.736
Weibull		5.354	5.649	6.182	6.777	7.166	7.688	8.289	9.429	10.777	11.706

the quantiles of the log-Gumbel distribution (*LG*) and log-logistic distribution (*LL*) are greater than those of other distributions for any value of the coefficient of *L*-variation (τ). The relative differences growing with τ value and the influence of thick tail is much more pronounced for greater cumulative probability (*F*) value. For instance, for $\tau = 0.35$, the ratio of log-Gumbel quantile to log-normal quantile equals 1.3 and 2.2 for $F = 0.99$ and $F = 0.999$, respectively. Relations of τ and C_V for the distributions of Table 4 are displayed in Figure 3, while the relations of τ_3 and C_S are given in Figure 4.

For three-parameter distributions (Table 5, where $\lambda_1 = 0$, $\lambda_2 = 1$), the generalized log-logistic (*GLL*) and *GEV* quantiles exceed the respective quantiles of thin-tailed distributions for any *L*-skewness coefficient value. Comparing with results of Table 4 one finds the difference in ranking of the distributions. Here *GLL* quantiles are greater than those of *GEV*. The relative differences between upper quantiles of heavy-tailed distributions and those of other distribution are growing both with the *L*-skewness (τ_3) value and the cumulative probability (*F*). Taking as the reference values those of Pearson (3) distribution, i.e., the distribution being still obligatory for FFA in Poland, we get for *GLL* and $\tau_3 = 0.33$ the ratio 1.2 and 1.8 for $F = 0.99$ and $F = 0.999$, respectively.

Concluding, the replacement of thin-tailed distributions by thick-tailed distributions, while using the *L*-moments estimation technique, gives rise to hydrologic design values, which are particularly significant for major structure designs. Surprisingly, the situation is a bit different, if the conventional moment technique is used instead of *L*-moments. The impact of heavy tails on the upper quantile estimates for both two-parameter distributions (Table 6) and three-parameter distributions (Table 7) is much less noticeable for MOM than when using the *L*-moment method and the differences in

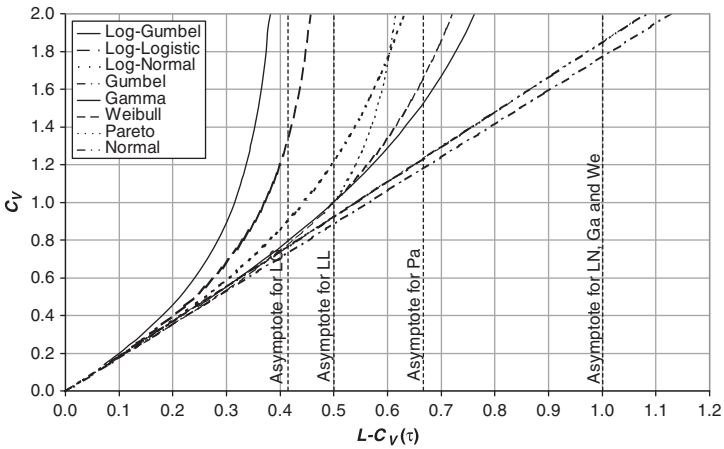

Figure 3 | The C_V - *L*-C_V relation for some two-parameter distributions. Note that (e.g. Hosking & Wallis 1997) $L\text{-}C_V \equiv \tau = \lambda_2/\lambda_1$ where $\lambda_2 = \int_0^1 x(F)(2F-1)dF$ and $\lambda_1 = \int_0^1 x(F)dF$.

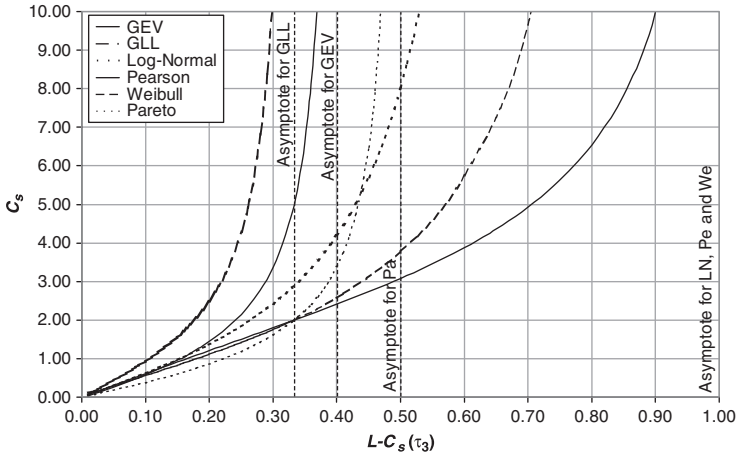

Figure 4 | The C_S – L-C_S relation for some three-parameter distributions. Note that (e.g. Hosking & Wallis 1997) $\tau_3 = \lambda_3/\lambda_2$ where $\lambda_3 = \int_0^1 x(F)(6F^2 - 6F + 1)dF$ and $\lambda_2 = \int_0^1 x(F)(2F - 1)dF$.

quantile values of various distributions are much smaller. Although for $C_V = 0.3$ and 0.6 the values of *LG* and *LL* are still the largest of all presented here (Table 6), for $C_V = 1.0$ and 1.5 both *LG* and *LL* produce lower values for $F = 0.99$ than all other distributions but the normal and Gumbel for $C_V = 1.0$. For $C_V = 1.0$, for instance, $x_{F=0.99}$ of the log-Gumbel is 85% of the log-normal value. As before, the influence of thick tail is more pronounced for greater cumulative probability (F) value. For $F = 0.999$, which corresponds to a major structure design value, it is only for $C_V = 1.5$ where the both log-normal and inverse Gaussian quantiles are greater than those of the heavy-tailed distributions.

For three-parameter distributions (Table 7, where $\alpha_1 = 0$, $\sigma = 1$) and $F = 0.99$, the values of *GEV* and *GLL* quantiles are generally less than those of thin-tailed distributions. For $F = 0.999$ the quantiles of heavy-tailed distributions exceed those of thin-tailed distributions only for small skewness, i.e., for $C_S \leq 2$. Note that the quantiles for given C_S differ less than those of L-moments for given L-C_S, pointing to greater robustness of MOM large quantiles to a distribution function. Moreover, note that the *GEV* quantiles are greater than those of *GLL*, while quantiles from L-moments show an opposite order. Concluding, the replacement of thin-tailed models by heavy-tailed models, while using MOM, does not have so significant an effect on hydrologic design value, in particular for three-parameter models as if LMM was applied.

While designing major dams and nuclear power facilities, the issue facing engineers is the reliability of estimation over the 500-year flood. Dealing with PDF having unlimited upper

Table 6 | Upper quantiles vs. the coefficient of variation. Two-parameter distributions and the method of moments while the mean: $\alpha_1 = 100$

	$x_{F=0.99}$				$x_{F=0.999}$			
PDF C_V	**0.3**	**0.6**	**1**	**1.5**	**0.3**	**0.6**	**1**	**1.5**
Log-Gumbel	210.03	318.34	416.74	480.49	327.75	653.17	1037.31	1334.97
Log-Logistic	197.59	312.89	433.70	518.74	284.12	592.60	1022.49	1396.72
Log-normal	189.62	311.51	490.49	693.30	237.28	475.80	926.47	1588.88
Inverse Gaussian	189.05	309.78	498.41	748.09	233.86	448.39	835.49	1436.13
Gumbel	194.10	288.20	413.67	570.50	248.07	396.13	593.55	840.33
Gamma	182.65	288.97	460.52	707.71	218.67	388.90	690.78	1172.86
Weibull	167.12	272.93	460.54	719.24	186.40	345.62	690.83	1300.25
Normal	169.79	239.58	332.63	448.95	192.71	285.41	409.02	563.54

Table 7 | Upper quantiles vs. the coefficient of skewness. Three-parameter distributions and the method of moments while the mean: $\alpha_1 = 0$ and the standard deviation $\sigma = 1$

		$x_{F=0.99}$					$x_{F=0.999}$				
PDF	C_S	**1.14**	**1.5**	**2**	**3**	**5**	**1.14**	**1.5**	**2**	**3**	**5**
GEV		3.140	3.313	3.479	3.640	3.707	4.947	5.582	6.330	7.340	8.139
GLL		3.092	3.226	3.416	3.455	3.535	5.487	6.018	6.973	7.225	7.962
Log-normal		3.117	3.310	3.519	3.779	3.959	4.930	5.509	6.242	7.418	8.880
Inverse Gaussian		3.123	3.336	3.594	3.984	4.383	4.832	5.373	6.085	7.355	9.346
Pearson (3)		3.112	3.330	3.605	4.051	4.573	4.730	5.234	5.908	7.152	9.220
Weibull		3.090	3.327	N.A.*	N.A.	N.A.	4.553	5.130	N.A.	N.A.	N.A.

*N.A. – not available

tail, the extrapolation enters an "impossible" zone, i.e., beyond the presumable Probable Maximum Flood (PMF). However, the definition of PMF is really rather vague and methods allowing better estimates of this bound should be developed. A promising area for research is the use of atmospheric models. According to Kuchment (2008), the PMF of large Russian rivers can be estimated assuming the maximum possible snow-melting intensity lasting for the concentration time, and no losses for infiltration.

LOOKING FOR HEAVY-TAILED DISTRIBUTIONS OF POLISH RIVER FLOW DATA

As a case study, time series of annual maxima from 39 gauging stations in Poland (see Figure 5 and Table 8) were analysed. In general, the data cover the period 1921–2006 (86 years), a few series being shorter, i.e., 70 years, from the period 1921–1990. The gauges encompass catchments of different areas (from 58.4 km^2 for Zakopane-Harenda on the Biały Dunajec River to 194,376 km^2 for Tczew on the Vistula River) and are located along rivers representing a wide range of hydromorphological conditions and flow regimes: from the mountainous (the Biały Dunajec, the Dunajec, the San, upper Vistula and its tributaries) to upland (the Warta at Poznan) and lowland (the Bug). The range of observed maximum flows varied from 195 m^3/s for Zakopane to 9,550 m^3/s for Tczew on the Vistula River. Though the number of gauges is significant, they are not fully representative of the Polish hydrological regime. One can see (Figure 5) that most of the gauges are concentrated in the southern, mountainous part of Poland. Nevertheless, this part of Polish territory shows strong flood potential and for this reason FFA is of great importance there.

In the twentieth century, according to Polish hydrological regulations, peak flows for a given probability of exceedance were calculated assuming (for all sites) a Pearson (3) distribution function with parameters estimated by means of quantile methods and by MLM for major structures (CUGW 1969). Recently, however, a seasonal approach has been implemented at the Institute of Meteorology and Water Management (Poland). The type of winter/summer distribution was selected from a four-element set of candidates using the AIC criterion. However, this approach is not obligatory and in many applications Pearson (3) is still used.

While scrutinizing the data, the feasibility of modelling each time series by a unimodal PDF should be evaluated. Therefore, the visual assessment of nonparametric kernel PDFs (Adamowski 1985; Adamowski & Feluch 1990; Lall *et al.* 1993) was carried out. Despite the fact that Polish annual peak flow series are mixtures of winter and summer peaks, their empirical probability density functions resemble unimodal distributions. As it was stated earlier, the distribution choice is crucial for a design value, i.e., for large quantiles estimation. To assess the fitness of various distributions to the data, the L-moment ratios are used as summary statistics, namely, coefficients of L-variation (L-$C_V \equiv \tau$), L-skewness (L-$C_S \equiv \tau_3$), and L-kurtosis (L-$C_K \equiv \tau_4$) were calculated for each of the 39 Polish gauges. They are listed in Table 8 and shown on the L-moment ratio diagrams together with relationships of various distributions, namely

- L-C_S vs L-C_V for 8 selected two-parameter models – Figure 6.
- L-C_K vs L-C_S for 7 three-parameter distributions – Figure 7.

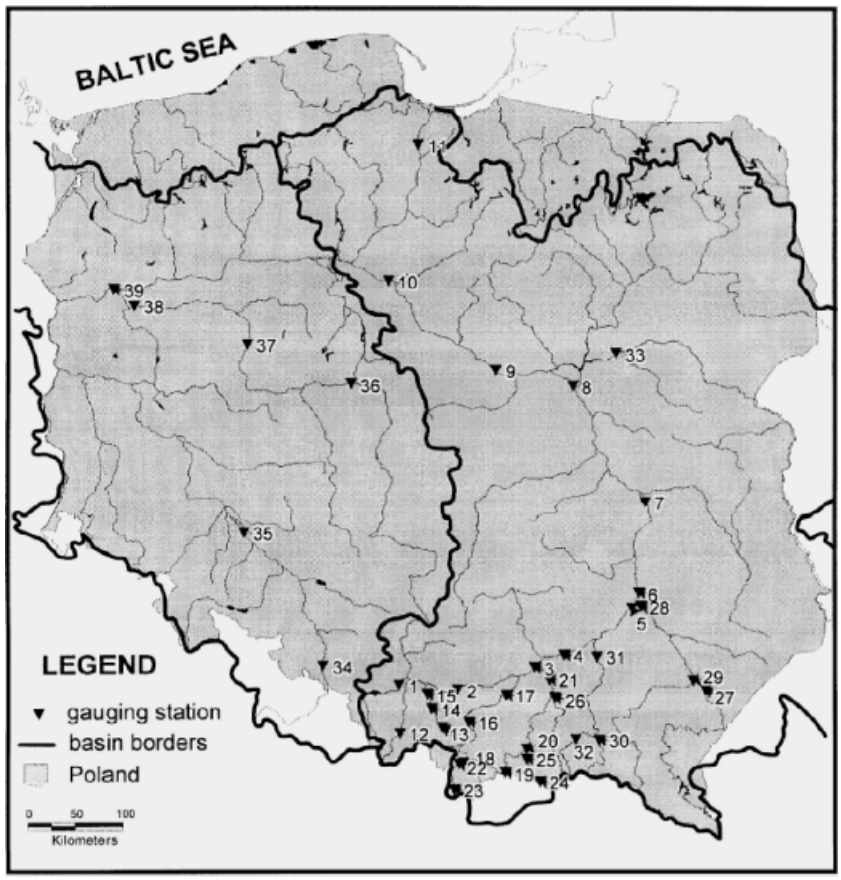

Figure 5 | Map of Poland with the 39 gauges.

As one can see, the allocation of the sampling points (marked by + or ●, the meaning of which will be explained later) is almost equally dispersed on the big part of the appropriate graph area and they cluster neither around one distribution type nor around a heavy-tailed distribution group.

Only a few points on both diagrams are located relatively close to the lines of heavy-tailed distributions: ten points for two-parameter distributions and nine for three-parameter distributions. Moreover, points showing heavy-tailed characteristics for two-parameter distributions do not fully coincide with those for three-parameter distributions. The rest of the points tend rather close to light-tailed distributions in Figure 6 and in Figure 7 as well. This means that according to visual assessment of the data location, the Polish annual peak flows, at least those considered in this study, should not be described by heavy-tailed distributions. The observed dispersion of points does not confirm the belief that all Polish annual maxima datasets follow the Pearson (3) distribution. Only seven points cluster around the Pearson (3) line (Figure 7).

On the other hand, in general, the points representing the gauges form similar structures for the same river reach. The strongest and quite stable patterns reveal subsequent reaches of the Vistula River on the three-parameter distribution graph (Figure 7). The first river reach of the upper Vistula (with the first gauge) is clearly the inverse Gaussian model; the next two gauges along the river (nos. 2 and 3) follow the same theoretical line, i.e., log-normal; the next three gauges (nos. 4 and 5), located downstream on the Dunajec River – a large tributary significantly influencing the Vistula's flood magnitude – are also close to the same theoretical line (Generalized Pareto). Further downstream we can recognise the Vistula's reaches as Weibull (gauge nos. 6–9), whereas the final two gauges are clearly identified by *GEV* distribution. Surprisingly, when floods on the main river and its tributary are not of the same origin (for example, one is of summer and the

Table 8 | Origin and characteristics of flood data considered

	Gauging station		Drainage area	Average peak flow	Winter floods share
Basin/River	No.	Name	(10^3 km^2)	(m^3/s)	(%)
Vistula	1	Jawiszowice	0.971	149.4	25.7
	2	Tyniec	7.52	719.1	40.0
	3	Jagodniki	12.1	1126	44.3
	4	Szczucin	23.9	1906	44.3
	5	Sandomierz	31.9	2485	51.4
	6	Zawichost	50.7	3281	52.9
	7	Pulawy	57.3	3004	57.1
	8	Warsaw	84.5	2998	62.9
	9	Kepa	169	3937	71.4
	10	Torun	181	3917	74.3
	11	Tczew	194	3963	77.1
Vistula/Sola	12	Zywiec	0.785	301.4	25.7
Vistula/Skawa	13	Sucha	0.468	153.5	30.0
	14	Wadowice	0.835	256.8	32.9
Vistula/Skawa/Wieprzowka	15	Rudze	0.154	53.0	45.7
Vistula/Raba	16	Stroza	0.644	219.0	31.4
	17	Proszowki	1.47	459.8	32.9
Vistula/Dunajec	18	Kowaniec	0.681	250.9	42.9
	19	Kroscienko	1.58	458.7	20.0
	20	Nowy Sacz	4.34	933.6	31.4
	21	Zabno	6.74	1161	32.9
Vistula/Dunajec/ Czarny Dunajec	22	Nowy Targ	0.432	172.2	32.9
Vistula/Dunajec/Bialy Dunajec	23	Zakopane	0.058	37.9	27.1
Vistula/Dunajec/Poprad	24	Muszyna	1.51	228.1	55.7
	25	Stary Sacz	2.07	319.0	48.6
Vistula/Dunajec/Biala	26	Koszyce W.	0.957	267.4	40.0
Vistula/San	27	Jaroslaw	7.04	794.1	64.3
	28	Radomysl	16.8	985.2	65.7
Vistula/San/Wislok	29	Tryncza	3.52	240.4	68.6
Vistula/Wisloka	30	Zolkow	0.581	167.2	44.3
	31	Mielec	3.69	545.0	52.9
Vistula/Wisloka/Ropa	32	Kleczany	0.482	114.7	32.9
Vistula/Bug	33	Wyszkow	39.1	667.3	95.7
Oder	34	Miedonia	6.74	557.8	25.0
	35	Trestno	20.4	1342	45.6
Oder/Warta	36	Konin	13.4	255.4	84.3
	37	Poznan	25.9	378.4	88.6
	38	Skwierzyna	32.1	416.1	94.3
	39	Gorzow	52.4	545.8	94.3

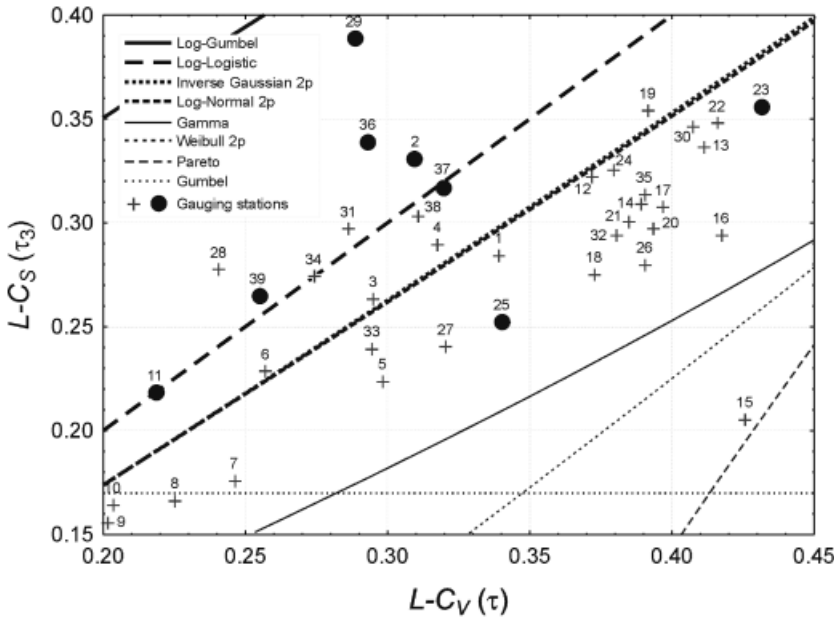

Figure 6 | The $L\text{-}C_V - L\text{-}C_S$ for 39 gauging sites in Poland.

other of winter origin or vice versa) changes in the distribution type are not as clearly noticeable as for a catchment characterized by common flood origins.

To back up the visual observations and to select heavy-tailed datasets, the two-step procedure of model selection (El Adlouni *et al*. 2008) was applied. Firstly, with the help of HYFRAN software, log–log plots for each Polish peak flow sample were constructed. Only eight datasets were classified as C class, i.e., regularly varying distributions: Fréchet ($EV2 =$ special case of heavy-tailed GEV distribution),

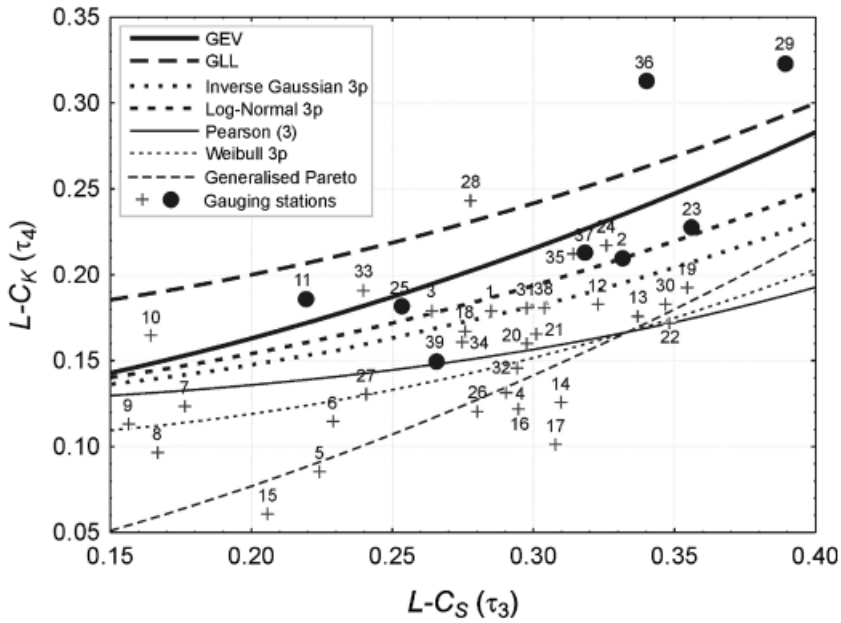

Figure 7 | The $L\text{-}C_S - L\text{-}C_K$ for 39 gauging sites in Poland.

Halphen IB (*HIB*), log-Pearson (3) (*LP3*), inverse gamma (*IG*). These datasets are marked in Figures 6 and 7 by black dots (●) and being candidates for a heavy-tailed sample indeed concentrate close to the heavy-tailed *L*-moments ratios lines – regardless of whether they are two- or three-parameter distributions.

The next step was to test which of the four regularly varying distributions best describe datasets qualified as class C; to do so, the BIC and AIC criteria were calculated for each C-class dataset. According to both criteria, the heavy-tailed inverse gamma distribution fitted best to five peak flow series, i.e., nos. 2, 11, 29, 36 and 39, out of eight belonging to class C. Only two gauges (nos. 23 and 25) are best described by log-Pearson (3) distribution and one (no. 37) by the heavy-tailed Fréchet (*GEV*) distribution. Eventually, one can say that only 8 out of 39 peak flow series (20%) revealed heavy-tailed extreme value nature. These gauges represent both large and small, mountainous and low-land rivers, so to summarize, the Polish datasets should be characterised by light-tailed distributions rather than by heavy-tailed distributions. This result and conclusion may however be due to rather short time series. Apart from *L*-moment properties, only exceptionally long data series make it possible to capture the effect of the distribution tail, but in hydrology the exceptionally long and homogeneous time series have "fairy tail", sorry, "fairy tale" character.

CONCLUSIONS AND RECOMMENDATIONS

Since the assumptions of extreme value theory are irrelevant for flood events, there is little use of it for realistic FFA. Consequently, the theoretical asymptotic extreme value distributions should be considered only as alternatives to other distributions, while the eventual choice of the distribution should be based on purely empirical fitting. Nowadays, there is a growing conviction that hydrological extremes are heavy-tail distributed. Several one- and two-shape parameter heavy-tailed distributions are derived by transformation of some soft-tailed distributed variables or both soft- and heavy-tailed distribution functions. Moreover, there exists a class of long-tail distributions without restriction on the existence of moments (Czechowski 2005). They are derived from power transformation $y = x^k$ for sufficiently large k of exponentially, Gamma (Krickiy & Menkel 1950) or inverse Gaussian (Strupczewski *et al.* 2008) distributed variables.

However, the power of discrimination procedures of distributions is very low for hydrological sample sizes (30–70 elements), while the effect of the model selection is more critical in the upper tail of distribution. The use of several discrimination procedures supplemented by the classical graphical analysis on a probability paper is advisable. Although upper elements of annual peak flow samples are usually highly error corrupted, nowadays special attention is paid to the fidelity of tail reproduction (e.g., Moon & Lall 1994; El Adlouni *et al.* 2008). The estimation of tail behaviour may be a fundamentally different problem than that of estimating a suitable density function for the main body of the data. The *L*-moment method can be recommended for the estimation of model parameters, as it gives much lower model bias of upper quantile estimates than the ML method. In accordance with expectation, the *L*-moment estimates of upper quantiles are greater for heavy-tailed distributions than those of other alternative distributions, which is not always observed when the method of moments is applied. Therefore, the replacement of thin-tailed models by thick-tailed models, while using the *L*-moment estimation technique, gives rise to hydrologic design values, which is particularly significant for major structure designs.

Investigation of Polish annual maxima datasets by the *L*-moment ratio diagrams for two- and three-parameter distributions and by the two-step procedure of model selection (El Adlouni *et al.* 2008) shows that they follow light-tailed distributions rather than heavy-tailed distributions. Only 9 out of 39 stations are located relatively close to lines of heavy-tailed distributions on the $L\text{-}C_S$–$L\text{-}C_K$ moment ratio diagram, while the linearity hypothesis of the log–log plot was verified at the 5% significance level for 8 of 39 datasets only. The $L\text{-}C_S$–$L\text{-}C_K$ diagram points to the three-parameter inverse Gaussian as the best fitted of distributions considered for a majority of Polish data sets, i.e., distributions with more light tail than that of the log-normal distribution. The long-tailed distributions obtained by the *Tx* transformation of the gamma or inverse Gaussian may be considered as alternatives for the heavy-tailed models for Polish rivers.

Concluding, the impossibility of "true" model identification even if it is of a simple form, sample constraints in multi-parameter estimation, the assessed magnitude of the

model error of upper quantile estimation, the non-stationarity of river flow process, and problems of ungauged catchments lead to the conclusion that we should step back and focus on the physics of extremes in hydrology.

ACKNOWLEDGEMENTS

We greatly appreciate the thoughtful comments of the anonymous reviewers. This work was partly financed by the Polish Ministry of Science and Higher Education under the Grant 0920/B/P01/2009/37 titled *Implementation of new parametric methods for hydrological design in time-variant environment* and COST Action ES0901 titled *European Procedures for Flood Frequency Estimation (FloodFreq)*. The authors would like to express their gratitude to M.Sc. A. Kozlowski for initial analysis of Polish datasets.

REFERENCES

Adamowski, K. 1985 Nonparametric kernel estimation of flood frequencies. *Water Resour. Res.* **21**(11), 1585–1590.

Adamowski, K. & Feluch, W. 1990 Nonparametric flood-frequency analysis with historical information. *J. Hydraul. Engng.* **116**(8), 1035–1047.

Akaike, H. 1970 Statistical predictor identification. *Ann. Inst. Statist. Math.* **22**, 203–217.

Cox, D. R. & Miller, H. D. 1965 *The Theory of Stochastic Processes*. Chapman and Hall, London.

CUGW 1969 Zasady obliczania największych przepływów rocznych o określonym prawdopodobienstwie pojawienia sie (*Principle of calculation of annual peak flows for a given probability of exceedance*). Centralny Urzad Gospodarki Wodnej, Wydawnictwo Katalogow i Cennikow (in Polish).

Cunnane, C. 1989 Statistical distributions for flood frequency analysis. *Operational Hydrology Report No. 33*, WMO, Geneva, Switzerland, pp. 73 + 6 Appendices.

Czechowski, Z. 2001 Transformation of random distributions into power-like distributions due to non-linearities: application to geophysical phenomena. *Geophys. J. Int.* **144**, 197–205.

Czechowski, Z. 2005 The importance of the privilege in resource redistribution models for appearance of inverse-power solutions. *Physica A* **345**, 92–106.

Dooge, J. C. I. 1973 Linear theory of hydrologic systems. *Techn. Bull. 1468*, Agricultural Research Service, Washington, DC.

El Adlouni, S., Bobée, B. & Ouarda, T. 2008 On the tails of extreme event distributions in hydrology. *J. Hydrol.* **355**, 16–33.

Griffis, V. W. & Stedinger, J. R. 2007 The LP3 distribution and its application in flood frequency analysis, 1. Distribution Characteristics. *J. Hydrol. Engng.* **12**(5), 482–491.

Hayami, S. 1951 On the propagation of flood waves. *Kyoto Univ. Japan, Disaster Prevention Res. Inst. Bull.* **I**, 1–16.

Hosking, J. R. M. & Wallis, J. R. 1997 *Regional Frequency Analysis*. Cambridge University Press, Cambridge.

Hurvich, C. M. & Tsai, C.- L. 1989 Regression and time series model selection in small samples. *Biometrika* **76**(2), 297–307.

Katsnelson, J. & Kotz, S. 1957 On the upper limit of some measures of variability. *Archiv. F. Meteor. Geophys. u. Bioklimat. B* **8**, 103.

Khaliq, M. N., Ouarda, T. B. M. J., Ondo, J. C., Gachon, P. & Bobée, B. 2006 Frequency analysis of a sequence of dependent and/or non-stationary hydro-meteorological observations: A review. *J. Hydrol.* **329**, 534–552.

Kirby, W. 1974 Algebraic boundedness of small samples. *Water Resour. Res.* **10**(2), 220–222.

Klemeš, V. 2000 Tall tales about tails of hydrological distributions. II. *J. Hydrol. Engng.* **5**(3), 232–239.

Krickiy, S. N. & Menkel, M. F. 1950 *Hydrologic Foundations of River Hydro Engineering*. In Russian, Izdatel'stvo Akademii Nauk SSSR, Moscow.

Kochanek, K., Strupczewski, W. G., Singh, V. P. & Węglarczyk, S. 2005 Are parsimonious FF models more reliable than true ones? II. Comparative assessment of the performance of simple models versus the parent distributions. *Acta Geophys. Pol.* **53**(4), 437–457.

Kuchment, L. S. 2008 *River Runoff (Genesis, Modelling, Predictions)*. In Russian, Ch. 8. Academy of Sciences, Water Problems Institute, Moscow.

Kuczera, G. 1982 Robust flood frequency models. *Water Resour. Res.* **18**(2), 315–324.

Lall, U., Moon, Y.-I. & Bosworth, K. 1993 Kernel flood frequency estimators: bandwidth selection and kernel choice. *Water Resour. Res.* **29**(4), 1003–1015.

Landwehr, J. M., Matalas, N. C. & Wallis, J. R. 1980 Quantile estimation with more or less floodlike distributions. *Water Resour. Res.* **16**(3), 547–555.

Leadbetter, M. R., Lindren, G. & Rootzén, H. 1983 *Extremes and Related Properties of Random Sequences and Processes*. Springer, New York.

Madsen, H., Rasmussen, P. V. & Rosbjerg, D. 1997 Comparison of annual maximum series and partial duration series methods for modeling extreme hydrologic events. I At-site modeling. *Water Resour. Res.* **33**(4), 747–757.

Makkonen, L. 2008 Problems in the extreme value analysis. *Structural Safety* **30**, 405–419.

Malamud, B. D. & Turcotte, D. I. 2006 The applicability of power-law frequency statistics to flood. *J. Hydrol.* **322**, 168–180.

Markiewicz, I. & Strupczewski, W. G. 2008 Simulation approach used for the second *L*-moment derivation. In: *Publ. Inst. Geophys. PAS E-10(406)* Rowiński, P. M. (Ed.), pp. 109–116.

McCauley, J. L. 1995 *Chaos, Dynamics and Fractals. An Algorithmic Approach to Deterministic Chaos*. Cambridge University Press, Cambridge.

Mitosek, H. T., Strupczewski, W. G. & Singh, V. P. 2006 Three procedures for selection of annual flood peak distribution. *J. Hydrol.* **323**(1–4), 53–73.

Moon, Y. & Lall, U. 1994 Kernel quantile function estimator for flood frequency analysis. *Water Resour. Res.* **30**(11), 3095–3103.

NERC, 1975 *Flood Studies Report*. Natural Environment Research Council, London.

Newman, M. E. J. 2005 Power laws, Pareto distributions and Zipf's law. *Contemp. Phys.* **46**, 323–351.

Perreault, L., Bobee, B. & Rasmussen, P. F. 1999 Halphen distribution system. I: Mathematical and statistical properties and II: Parameter and quantile estimation. *J. Hydrol. Engng ASCE* **4**(3), 189–199, 200–208.

Rao, A. R. & Hamed, K. H. 2000 *Flood Frequency Analysis*. CRC Press, Boca Raton, FL.

Robson, A. & Reed, D. 1999 *Flood Estimation Handbook*. Vol 3. Statistical Procedures for flood frequency estimation. Institute of Hydrology. Crowmarsh Gifford. Wallingford, Oxfordshire, UK.

Rosbjerg, D., Madsen, H. & Rasmussen, P. F. 1992 Prediction in partial duration series with generalized Pareto-distributed exceedance. *Water Resour. Res.* **28**(11), 3001–3010.

Sankarasubramanian, A. & Lall, U. 2003 Flood quantiles in a changing climate: Seasonal forecasts and causal relations. *Water Resour. Res.* **39**(5), 1134, 4. 1–11.

Schwarz, G. E. 1978 Estimating the dimension of a model. *Ann. Stat.* **6**(2), 461–464.

Stedinger, J. R. & Griffis, V. W. 2008 Flood frequency analysis in the United States: Time to update. Editorial. *J. Hydrol. Engng.* **13**(4), 199–204.

Strupczewski, W. G. 1964 Rownanie fali powodziowej (*Flood hydrograph equation*). In Polish, Warsaw. *Wiad. Sl. Hydrol. Meteorol.* **57**(2), 35–58.

Strupczewski, W. G. & Kaczmarek Z. 2001 Non-stationary approach to at-site flood-frequency modelling. Part II. Weighted least squares estimation. *J. Hydrol.* **248**, 143–151.

Strupczewski, W. G. & Kochanek, K. 2009 The study on application of log-inverse Gaussian distribution function in hydrology of Polish rivers. *Unpublished Memorandum PAS 28/1/2009*, Institute of Geophysics.

Strupczewski, W. G., Kochanek, K., Feluch, W., Bogdanowicz, E. & Singh, V. P. 2009 On seasonal approach to nonstationary flood frequency analysis. *Phys. Chem. Earth* **34**(10–12), 612–618.

Strupczewski, W. G., Kochanek, K., Singh, V. P. & Weglarczyk, S. 2005 Are parsimonious FF models more reliable than true ones? I. Accuracy of quantiles and moments estimation (AQME) – Method of assessment. *Acta Geophys. Pol.* **53**(4), 419 –436.

Strupczewski, W. G., Markiewicz, I., Kochanek, K. & Singh, V. P. 2008 Short walk into two-shape parameter flood frequency distributions. In *Hydrology and Hydraulics* (Singh V. P. ed), Water Resources Publications. Ch. 19, pp. 669–688.

Strupczewski, W. G., Mitosek, H. T., Kochanek, K., Singh, V. P. & Weglarczyk, S. 2006 Probability of correct selection from Log-normal and Convective Diffusion models based on the likelihood ratio. *SERRA* **20**, 152–163.

Strupczewski, W. G., Singh, V. P. & Feluch, W. 2001*a* Non-stationary approach to at-site flood-frequency modelling. Part I. Maximum likelihood estimation. *J. Hydrol.* **248**, 123–142.

Strupczewski, W. G., Singh, V. P. & Weglarczyk, S. 2001*b* Impulse response of Linear Diffusion Analogy model as a flood frequency probability density function. *Hydrol. Sci. J.* **46**(5), 761–780.

Strupczewski, W. G., Singh, V. P. & Weglarczyk, S. 2002*a* Asymptotic bias of estimation methods caused by the assumption of false probability distribution. *J. Hydrol.* **258**(1-4), 122–148.

Strupczewski, W. G., Singh, V. P. & Węglarczyk, S. 2002*b* Physics of flood frequency analysis. I. Linear convective diffusion wave model. *Acta Geophys. Pol.* **50**(3), 433–455.

Strupczewski, W. G., Singh, V. P., Węglarczyk, S. & Mitosek, H. T. 2003 Physics of flood frequency analysis. II. Convective diffusion model versus lognormal model. *Acta Geophys. Pol.* **51**(1), 85–106.

Strupczewski, W. G., Węglarczyk, S. & Singh, V. P. 2002c Model error in flood frequency estimation. *Acta Geophys. Pol.* **50**(2), 279–319.

Tweedie, M. C. K. 1957 Statistical properties of the inverse Gaussian distributions, I. *Ann. Math. Stat.* **28**, 362–363

U. S. Water Resources Council, 1982 Guidelines for determining flood flow frequency. *Bulletin 17B*. Hydrol. Subcom. Office of Water Data Coordination. US Geological Survey. Reston, VA, p.182.

Van Monfort, M. A. J. & Witter, J. V. 1986 The generalized Pareto distribution applied to rainfall depth. *Hydrol. Sc. J.* **31**(2), 151–162.

Wallis, J. R., Matalas, N. C. & Slack, J. R. 1974 Just a moment! *Water Resour. Res.* **10**(2), 211–219.

Wang, Q. J. 1997 LH Moments for Statistical Analysis of Extreme Events. *Water Resour. Res.* **33**(12), 2841–2848.

Wilkins, J. E. 1944 A note on skewness and kurtosis. *Ann. Math. Stat.* **15**, 333–335.

First received 29 May 2009; accepted in revised form 18 June 2010. Available online February 2011